Chapter2

Materials and Methods

This chapter deliberates the complete description of materials and experimental methodologies for the synthesis of various material AuNPs, Cur-AuNPs, CEO-*f* AuNP, Hydroxyapatite (HA), Gold/Silver bimetallic Nanoparticles (Au/Ag NPs) as well as (1-x) HA-x Au/Ag NPs, composites. The current chapter also discussed about various characterization techniques used to characterize the synthesized materials such as: for Phase evolution - XRD and FTIR whereas for microstructural characterization - TEM, SEM and EDX are demonstrated. Other used characterizations are UV-Visible spectroscopy, Zeta & DLS, TGA. Mechanical properties (hardness, fracture toughness, compressive strength and flexural strength), antibacterial response (quantitatively and qualitatively) and cellular response are also discussed. In addition to this, various biomedical applications are also discussed briefly, i.e.; antibacterial, antibiofilm, antioxidant, anticancerous, biocompatibility and tissue engineering.

2.1 Synthesis

2.1.1Synthesis of Gold Nanoparticles (AuNPs)

Synthesis of gold nanoparticles using PEI and organic reducing agent (cyclohaxanone) has been done as descried earlier with some modifications (Pandey et al., 2016 and Pandey et al., 2017).Briefly, aqueous solution of $HAuCl_4$ (100 µL of a 20 mM solution) and PEI (100 µL of a 15.5 mg/ mL solution), were placed in 2 mL glass vial, followed by the addition of ethylene glycol (775µL) and cyclohexanone (25µL). The reaction mixture

was continuously mixed on a magnetic stirrer at 60° C. Within 2-3 min the reaction mixture turns to ruby red colour that indicated the formation of AuNPs.

2.1.2 Synthesis of Curcumin conjugated AuNPs (Cur-AuNPs)

As prepared AuNPs (100 µL) and different amount of curcumin solution (5mM in ethanol) was mixed for 15, 30, 60, 120 min and overnight on a magnetic stirrer at 40-45° C for active conjugation of curcumin on AuNPs surface. The purification has been done for Cur-AuNPs employing ultra-centrifugal filter device (30 kDa, Amico®, Millipore, USA). The suspension was filled into the filter device and centrifuged (10,000 g for 15 min, repeated 5times with an interval of 15 min). Because the pore size of the polymer membrane was much smaller than native curcumin particles, the curcumin particles were retained in the filter device. Cur-AuNPs nano-suspension was collected as an ultrafiltrate in the centrifuge tube those were used for subsequent experiments.

2.1.3 Synthesis of clove essential oil functionalized AuNPs (CEO-*f*AuNP)

As prepared AuNPs (100 µL) and different amount of CEO (10, 20, 50, 100 µL) was mixed for 15, 30, 45, 60, 120 min and overnight on a magnetic stirrer at room temperature (28°C) for active functionalization of CEO on AuNPs surface.

2.1.4 Synthesis of Bimetallic Gold/Silver Nanoparticles (Au/Ag NPs)

To synthesize 3-APTMS functionalized Au-Ag bimetallic nanoparticles, the salts of Ag^{+} and Au^{3+} were simultaneously reduced and stabilized using 3-APTMS and formaldehyde. In a typical procedure, 1 mL of solution was prepared by mixing 0.4 mL solutions of $HAuCl_4$ (0.025 M) and 0.1mL solution of $AgNO_3$ (0.025 M) to 0.3 mL solutions of 3-APTMS (0.01 M). The resulting yellow solution was stirred vigorously over a vertex

cyclomixer for 30 sec. The solution was then subjected to reduction by adding a 0.2 mL of Formaldehyde. The resulting mixture was stirred over a vertex cyclomixer for 30sec. The mixture was left to stand in the dark at 45-60°C for 2-3 min. After this, the colour of the reaction mixture turned to dark yellowish-orange colour indicating the formation of bimetallic Au/Ag NPs.

2.1.5 Synthesis of Hydroxyapatite (HA)

The synthesis of HA has been done using well established co-precipitation method. CaO and H_3PO_4 were used as raw material. Figure 2.1 represents the synthesis flow chart for HA. Initially, CaO powder was weighed by weighing balance (Shimadzu) and kept it in oven at 100ºC for 6-8 h to remove the moisture of the powder. Dried powder was mixed with double ionized (DI) water. For 25 g batch, CaO and DI water have been taken to be 15.49 g and 750 ml, respectively. The mixing was done by magnetic stirrer at temperature of 80ºC.

9.5 ml of orthophosphoric acid (H_3PO_4) was diluted with 1000 ml of DI water. The diluted H_3PO_4 solution was poured in to funnel and arrange or stand over CaO solution beaker. Then, mix diluted H_3PO_4 solution was added drop wise in to CaO solution beaker. The entire mixing procedure takes about 3 – 4 h. The pH of the solution was maintained (> 8) throughout the mixing process. After the completion of mixing, the solution was kept for 1 day for precipitation. The precipitate was collected by filtration. The filtered precipitate was kept overnight at 100ºC in oven for drying.

Now, the dried powder was crushed into fine particle and calcined at 800ºC for 2 h. Eq. 2.1 shows the formation of HA after calcinations.

$$\mathbf{10\ CaO\ + 6\ H_3PO_4 \rightarrow Ca_{10}(PO_4)_6(OH)_2\ + 18\ H_2O} \qquad \mathbf{(2.1)}$$

The calcined powder was crushed further and characterized to confirm the formation of pure phase of HA.

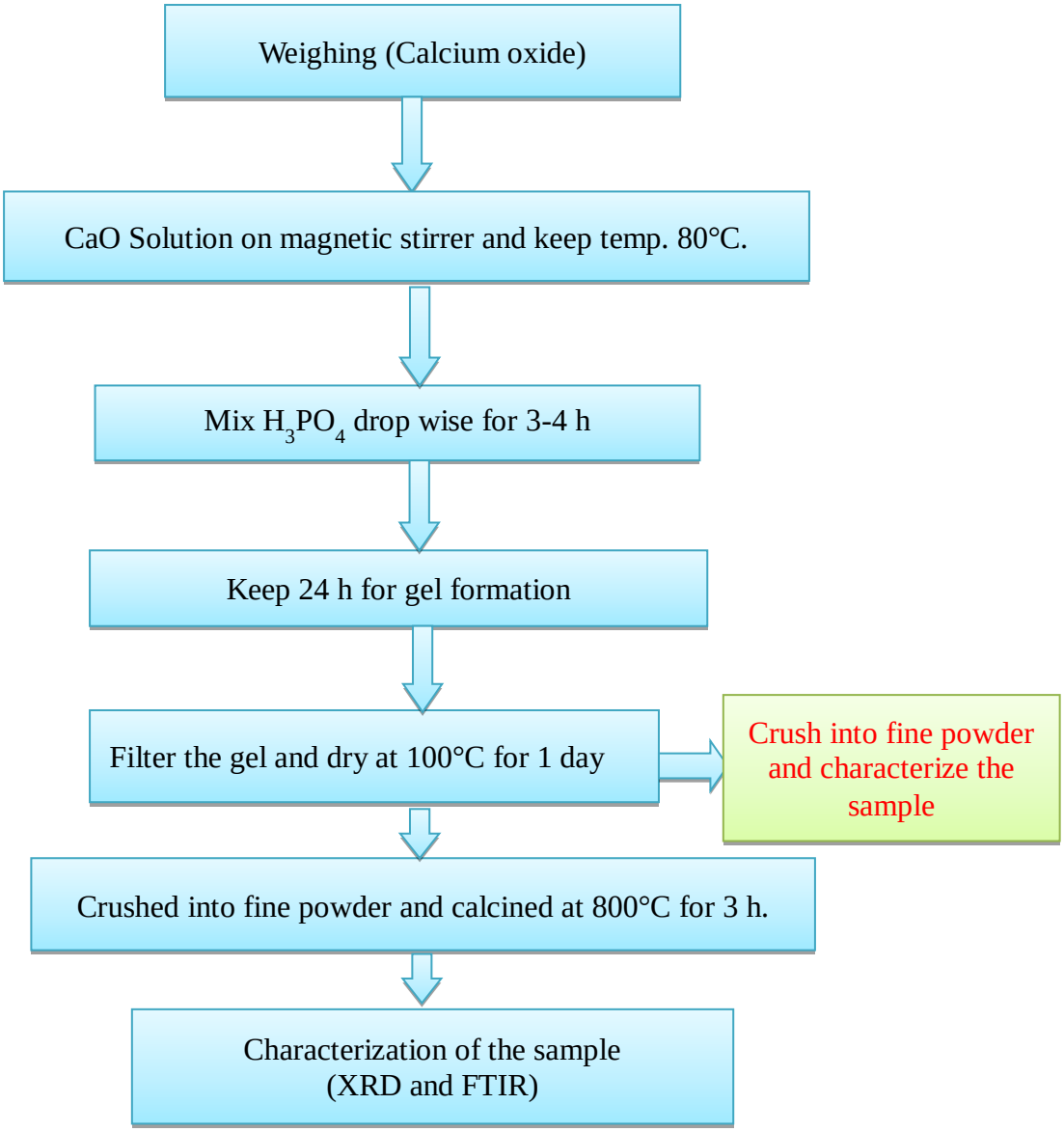

Figure 2.1 *Flow chart representing the synthesis of Hydroxyapatite (HA)*

2.1.6 Synthesis of (1-x) HA-x Au/Ag NPs Composites

(1-x) HA-x Au/Ag NPs (x= 2,5 and 10 wt. %) composite systems were fabricated via solid state synthesis route. The mixing of HA and Au/Ag NPs samples were done by ball

milling using zirconia balls (1:4 powder to ball ratio) and acetone (as milling media) in polyethylene jar for 24 h.

Table 2.1*Composition and nomenclature used for (1-x) HA-x Au/Ag NPs composites*

S. No.	HA (wt.%)	Au/Ag NPs (wt. %)	Nomenclature
1.	98	2	HA – 2Au/Ag NPs
2.	95	5	HA – 5Au/Ag NPs
3.	90	10	HA – 10Au/Ag NPs

The wet slurry of HA and Au/Ag NPs was kept overnight in oven for drying. The dried cake was crushed into fine particles. Table no. 2.1 shows the composition and nomenclature for (1-x) HA-x Au/Ag NPs which have been used throughout the thesis.

2.2Pelletization and sintering of composite samples

The pelletization of the powder samples was done by uniaxial hydraulic pressing at 5 MPa followed by cold isostatic pressing at 300 MPa.

Figure 2.2 *Composite samples after compaction*

The sintering temperature was optimized, based on the maximum densification as well as phase ratio. During optimization process, the samples were heated at heating rate of 5° / min. The optimized sintering temperature for (1-x) HA-x Au/Ag NPs composites is 1075°C for 2 h.

2.3 Characterizations

In this section, different methods employed for the characterization of the synthesized materials are demonstrated in subsequent sections. Techniques utilized for deciphering phase evolution include XRD and FTIR, while microstructural analysis is carried out through TEM, SEM, and EDX. Additionally, UV-Visible spectroscopy, Zeta & DLS, and TGA are enlisted as other pertinent characterizations.

2.3.1 UV Spectroscopic analysis

Ultra violet and visible (UV-Vis) absorption spectroscopy is the technique by which we measure attenuation of light which passes through a under consideration sample or also after reflection from the sample. Both parts (UV and Vis) of light are energetic that can excite electrons to higher energy levels (Chemicool Dictionary 2019). This follows the principle of the Beer-Lambert law which states that absorption of the light by the sample is directly proportional to the path length and concentration of the sample (Aman T. 2019).

Mathematically,

$$\mathbf{A=\log (I_0/I) = Ecl} \qquad \mathbf{(2.2)}$$

Where, A= absorbance, I_0= intensity of light incident upon sample cell, I= intensity of light leaving sample cell, C= molar concentration of solute, L= length of sample cell

(cm), E= molar absorptivity. When light falls on the sample each material absorbs a specific range of the light and shows the behavior accordingly. Electron from the atom excites towards the higher state from the lower energy state. The preliminary characterization of AuNPs/ Cur-AuNPs/ CEO-*f*AuNP was done by observing the UV-Vis spectrum using U-2900 UV-Vis spectrometer (Hitachi, Tokyo, Japan) over the scan range of 200-700 nm.

2.3.2 Zeta/ Dynamic Light Scattering (DLS)

Zeta potential is a measure of the effective electric charge on the nanoparticles surface. The magnitude of the zeta potential provides information about particle stability, particles with higher magnitude zeta potentials exhibiting more stability due to a larger electrostatic repulsion between particles. Zeta potential is a physical property exhibited by all solid-liquid and liquid-liquid colloidal systems. Surrounding the surface of all dispersed particles is a thin layer of ions that have the opposite charge of the particle's surface called the Stern layer. Further from the surface is an additional layer of more loosely-associated ions of opposite charge to the surface that move with the particle as it travels through a medium due to Brownian motion or sedimentation; this is called the double layer. The zeta potential is defined as the voltage at the edge of the slipping (shear) plane with respect to the bulk dispersing medium, where ions, molecules and other agents are no longer associated with a particle's surface. If two adjacent particles have sufficiently high zeta potentials of the same sign, they will not agglomerate due to repulsive electrostatic forces between particles with like charges.

Dynamic Light Scattering (DLS) measures the hydrodynamic diameter of nanoparticles in solution and provides information on the aggregation state of nanoparticles in solution.

The average particle size (hydrodynamic diameter), size distribution of the particle and Zeta potential measurements of synthesized AuNPs/ Cur-AuNPs/ CEO-*f*AuNP were performed using a Zetasizer instrument (Malvern Panalytical, Malvern, UK). The samples for analysis were prepared by diluting the colloidal aqueous solution of AuNPs/ Cur-AuNPs/ CEO-*f*AuNP with double distilled water, followed by sonication for 15 min.

2.3.3Density measurement

Densities of the sintered samples (HA and HA-x Au/Ag composites) were measured by Archimedes principal (Eq. 2.3).

$$\textbf{Densityofthebulksample}(\rho_{\textbf{actual}}) = \frac{\textbf{Dryweight}}{\textbf{Weightloss}} = \frac{W_1}{W_1 - W_2} \quad \textbf{(2.3)}$$

Where, Dry weight of the sample (in air) = W_1, Suspended weight (in water) = W_2.

Theoretical density

The theoretical densities for the composite samples were calculated using rule of mixture (Eq. 2.4).

$$\textbf{Theoreticaldensity}(\rho_{\textbf{th}}) = \frac{\rho_{\textbf{matrix}} V_{\textbf{matrix}} + \rho_{\textbf{secondaryphase}} V_{\textbf{secondaryphase}}}{V_{\textbf{matrix}} + V_{\textbf{secondaryphase}}} \quad \textbf{(2.4)}$$

Thus, densification can be obtained by (Eq. 2.5)

$$\textbf{Densification}(\%) = \frac{\rho_{\textbf{actual}}}{\rho_{\textbf{theoretical}}} \times 100 \quad \textbf{(2.5)}$$

2.3.4Phase evolution

2.3.4.1 X-ray Diffraction (XRD)

X-ray powder diffraction (XRD) is a rapid analytical technique primarily used for phase identification of a crystalline material and can provide information on unit cell

dimensions. X-ray diffraction is based on constructive interference of monochromatic X-rays and a crystalline sample. These X-rays are generated by a cathode ray tube, filtered to produce monochromatic radiation, collimated to concentrate, and directed toward the sample. The interaction of the incident rays with the sample produces constructive interference (and a diffracted ray) when conditions satisfy Bragg's Law ($n\lambda=2d \sin \theta$). This law relates the wavelength of electromagnetic radiation to the diffraction angle and the lattice spacing in a crystalline sample. These diffracted X-rays are then detected, processed and counted. By scanning the sample through a range of 2θangles, all possible diffraction directions of the lattice should be attained due to the random orientation of the powdered material. Conversion of the diffraction peaks to d-spacing allows identification of the mineral because each mineral has a set of unique d-spacing. Typically, this is achieved by comparison of d-spacing with standard reference patterns.

All diffraction methods are based on generation of X-rays in an X-ray tube. These X-rays are directed at the sample, and the diffracted rays are collected. A key component of all diffraction is the angle between the incident and diffracted rays.

X-ray diffraction (XRD) patterns of the AuNPs, Cur-AuNPs, CEO-*f*AuNP, HA and HA-x Au/Ag NPs composite samples were recorded using X-ray diffractometer (XRD, Rigaku Miniflex II Desktop X-ray Diffractometer) with Cu-Kα radiation (λ = 1.54056 Å).X-ray intensity was measured for angles in the range $20^o < 2\theta < 80^o$ with a step size of 0.05°and scan rate of 3° per minute. For identification of the phases, present in the sample, the diffraction patterns were then compared with the standard data in the JCPDS database using X pert high score software.

2.3.4.2 Fourier transform infrared (FTIR) Spectroscopy

Fourier transform infrared spectrometer (FTIR) is one of the instruments based on infrared spectroscopy. It is the most modern type and preferred over the other dispersive

spectrometers. It is because of its high precision, accuracy, speed, enhanced sensitivity, ease of operation, and sample non-destructiveness. The fundamental of infrared spectroscopic technology is on atomic vibrations of a molecule that only absorbs specific frequencies and energies of infrared radiation. The molecules could be detected and classified by FTIR because different molecules will have different infrared spectrum. The FTIR spectrometer essentially uses an interferometer to measure the energy that is being transmitted to the sample.

The Fourier transformation infrared spectroscopy (FTIR) measurement was carried out in order to analyze the presence of functional groups. The FTIR spectra were measured in transmission mode within the range of 4000 - 400 cm^{-1} with a FTIR spectrometer (Bruker Tensor 70).

2.3.5 Scanning Electron Microscopy (SEM) and Energy-dispersive X-ray spectroscopy (EDX)

Microstructural analyses were done using scanning electron microscope (SEM). It uses a focused beam of high-energy electrons in producing a variety of signals at the surface of specimen. The interacting electrons produced the signals which provide the information about the surface morphology etc. when the electron beam hits the surface, it may be either absorbed or reflected.

The magnification range may be from 30x to 500,000x. SEM (Zeiss, EVO 18 Research) is performed in the vacuum environment because air and water molecules can affect the electron beam. (Zhou et al., 1981).

2.3.6Transmission electron microscopy (TEM)

Transmission electron microscopy (TEM) is a form of microscopic analysis that transmits a high-energy beam of electrons through an ultrathin sample specimen. This

provides imagery based on the transmission/attenuation of electrons, which is then magnified for direct observation and analysis on the micro- and nano-scales.

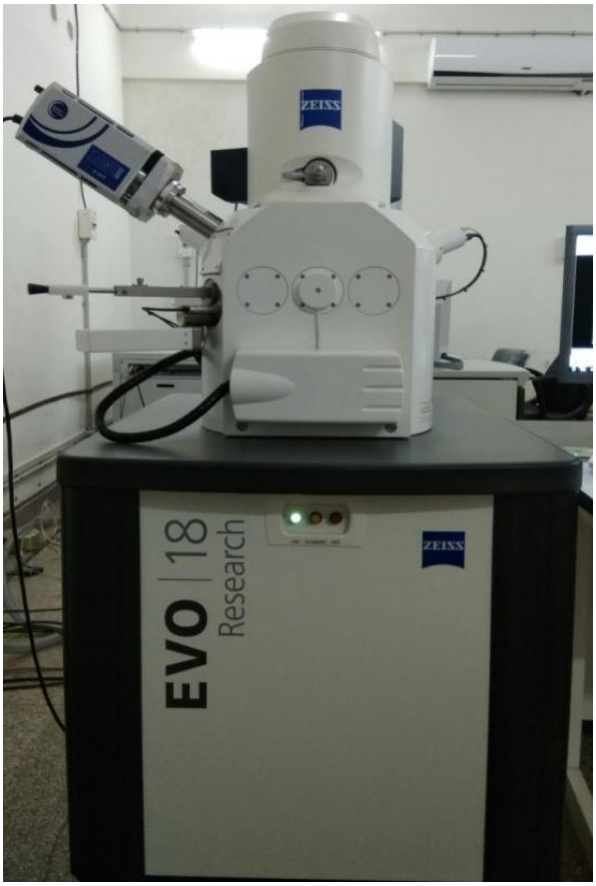

Figure 2.3 *Scanning Electron Microscope*

Figure 2.4 *Transmission Electron Microscope*

It is a very high-resolution technique for mapping a samples size, shape, and elemental structure in the nanometer size range. Transmission electron microscopy allows direct observation of a sample's structure and morphology at an atomic level, lower than a single nanometer.

Transmission electron microscopy operates using three primary components: an electron source; a series of electromagnetic lenses; and a sensitive optical detector. The high-voltage electron gun directs a beam of accelerated electrons through a condenser aperture, which focuses the beam onto the ultra-thin sample. Transmitted electrons imprint an image based on the distinct optical characteristics of the sample onto a photosensitive screen. This screen then emits photons that are acquired and imaged using a high-resolution camera.

TEM was applied to study the morphology, size and size distribution of the synthesized particles. TEM and selected area electron diffraction (SAED) analysis was carried out using a Tecnai G2 20 Twin instrument (FEI, Hillsboro, OR, USA) at the IIT (BHU) Central Instrumentation Facility. Samples were prepared by diluting the AuNPs, Cur-AuNPs and CEO-*f*AuNP in ethanol and drop casting the solution on carbon-coated copper grids.

2.4Mechanical characterization

2.4.1 Vicker's Hardness measurement

Hardness is the resistance of the material to plastic deformation and measured by standard indentation hardness test (Johnson 1970). The hardness of samples with 10 mm of diameter and 1.5 mm of thickness was measured by Vicker's hardness testing machine. This method consists of indenting the test material with a with pyramidal shaped diamond indenter. The indents were taken on the well-polished surfaces of the

pellets with Vicker's diamond pyramid indenter (Digi-test, VTP-6046) at room temperature with 1 kgf of load with 10 s dwell time (Figure 2.5).

The polishing process included grinding of the pellets on grinding papers with grades, 400-800,600-1200 and 2000. Finally, the samples were mirror polished using diamond polishing unit. Number of indents was taken on each sample. Vickers hardness (HV) was determined according to the method, described as ASTM E384 (ASTM 1984) and calculated by the formula (Eq.2.6),

$$\mathbf{HV = 1.854\ {}^{F}/_{d^2}} \qquad \mathbf{(2.6)}$$

Where, F is the load or force, applied to the diamond indenter in kilograms-force (kgf), d is the average length of the two diagonals.

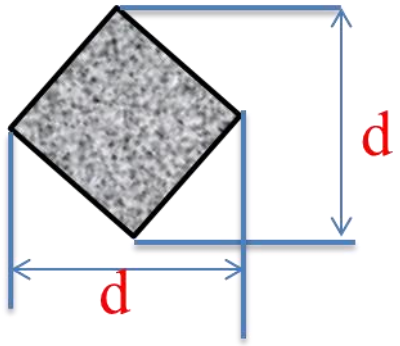

Figure 2.5 *Schematic diagram for indentation on the specimen at 1 kgf load with 10 s dwell time*

2.4.2 Fracture Toughness

Indentation method was used for calculating the fracture toughness of the disc samples with dimension of 10 mm × 1.5 mm. In this technique, crack lengths and crack radius of multiple indents were observed using SEM. Figure 2.6 shows the schematic diagram for indentation by pyramidal indenter at 5 kgf load and the dwell time was 10 s.

The fracture toughness (K_C) is evaluated by using Evans and Charles formula (Eq. 2.7) (Evans et al 1976),

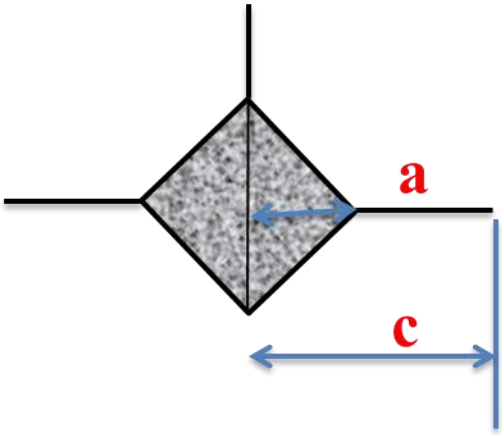

Figure 2.6 *Schematic diagram for crack generation on the specimen at 5 kgf load for 10s dwell time*

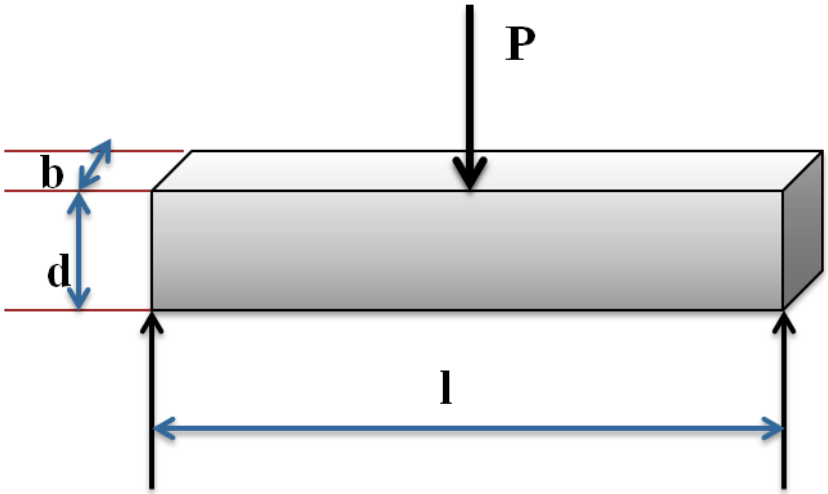

Figure 2.7 *Three point Flexural test*

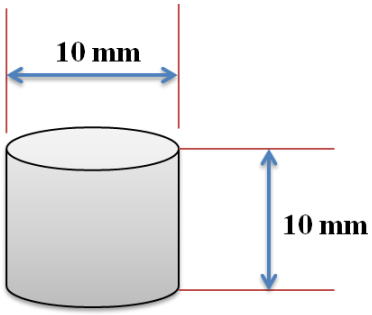

Figure 2.8 *Compressive test*

$$K_C = \frac{0.15\, k\, H}{\phi\sqrt{a}} (C)^{-3/2} \quad (2.7)$$

Where,

k is correction factor (i.e, k = 3.2 for C/a values ≥ 2),H, C, ϕ and a are the hardness, crack length, constraint factor (ϕ =3), and indent radius, respectively.

2.4.3 Flexural Strength

Flexural strength was measured by three point bend test method using universal testing machine (UTM, TInius Olsen). The rectangular bar shaped sample of dimension of 30 mm × 5 mm × 5 mm with crosshead speed of 0.05 mm/min were fractured [Figure 2.7]. The flexural stress was calculated using the formula (Eq. 2.8) (He at el., 2009):

$$\sigma_f = \frac{3PL}{2bd^2} \quad (2.8)$$

Where,

σ_f is flexural strength, P is fracture load, L, b and d are span length, breadth and thickness of the specimen, respectively.

2.4.4 Compressive Strength

The compressive strength was measured using Universal testing machine (UTM, Tinius Olsen H10KL) at cross head speed of 0.05 mm/min. The diameter and thickness of the cylindrical samples was measured to be 10 mm and 10 mm, respectively [Figure 2.8].

2.5Antibacterial behaviour

2.5.1 Quantitative analysis

3-(4, 5-dimethylthiazol-2-yl)-2, 5-diphenyl tetrazolium bromide (MTT) assay of, HA and HA-xAu/Ag NPs composite samples was performed to observe the viability of the bacterial cells in terms of optical density against the gram positive (*Staphylococcus aureus*; MTCC 435) and gram-negative bacteria (*Escherichia coli*; MTCC 443). Both,

the bacterial cells were revived in Nutrient Agar growth media for 10 h at 37ºC, before seeding on the samples. After washing with phosphate buffer saline (1x PBS), HA and HA-x Au/Ag NPs samples were seeded with bacterial cells of 0.1 OD (200 µl per well) in 24 well plate and incubated for 6 h at 37ºC. The incubated samples were cleansed twice with 1x PBS and 500 µl of MTT was added in the well (MTT: PBS in the ratio of 1:10) and incubated further for 2 h to form farmazan crystals which were dissolved with dimethyl sulfoxide (DMSO) (van de Loosdrecht et al (1994).The optical density of the solution was measured by ELISA Micro plate reader at wavelength of 595 nm and statistical analyses were done by SPSS 20 software. For statistical analyses of measured mean optical density, ANOVA method using Tukey test has been adopted at statistical significant value, $p < 0.05$.

2.5.2 Live / dead assay

Live / dead assay of *S. aureus* and *E. coli* bacterial cells on HA and HA-x Au/Ag NPs samples was performed to observed the viability of bacterial cells after incorporation of Au/Ag NPs secondary phase. The samples were seeded with bacterial (*E. coli* and *S. aureus*) cells (200 µl per well with 0.1 OD) in 24 well plate and incubated at 37ºC for 7-8 h. All the cultured samples were washed twice with 1x PBS solution after stipulated incubation period. Following this, a mixture of Syto 9 and propidium iodide dyes with the ratio of 9:1 was added for 30-40 min to stain the live and dead bacterial cells on the samples. After that, the imaging of live and dead bacterial cells was performed using fluorescence microscopy.

2.5.3 Nitro blue tetrazolium (NBT) assay

Nitroblue tetrazolium (NBT) is a pale-yellow color water-soluble nitro-substituted aromatic tetrazolium compound. It is an artificial electron acceptor and NBT assay has been suggested to be a useful tool in the studies of free radicals (Zhang et al., 1993;

Esfandiari et al., 2003). The principle of the assay is that NBT enters within the targeted cells following their incubation in NBT solution. Within the cells, the interaction of NBT with superoxide disrupts the tetrazole ring and tetrazoinyl radical is generated, which subsequently dismutase to generate the purple/blue water insoluble and stable formazan crystals (Figure 2.9) (Esfandiari et al., 2003; Volk and Moreland, 2014; Stockert et al., 2018). The reduction product (formazan) can be measured by spectrophotometer or by microscopy (Volk and Moreland, 2014).

NBT assay was performed to evaluate the superoxide production (O_2^-) which is a type of reactive oxygen species (ROS). Both the *S. aureus* and *E. coli* bacterial cells were seeded on pre-sterilized HA and HA-xAu/Ag NPs composite samples and then incubated for 6 h under standard condition.

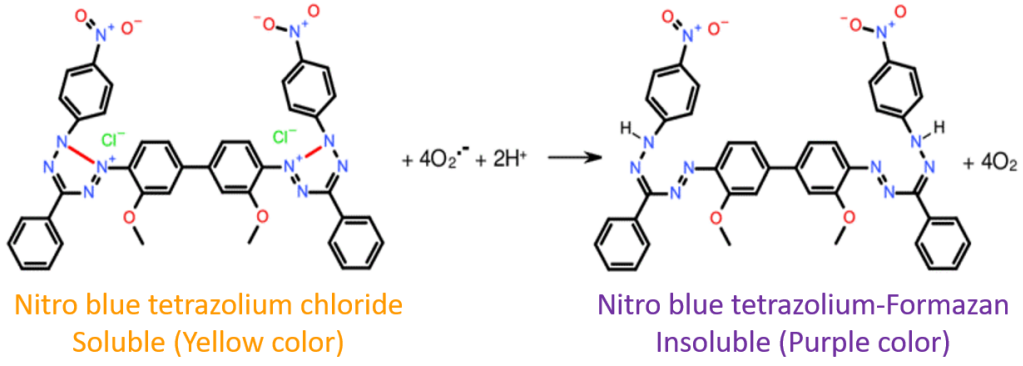

Figure 2.9 *Reaction mechanism of NBT with superoxide to form NBT-Formazan and diatomic*

After that 500 µl of NBT (10mg/ml in DI water) was added on the cultured samples and incubated further for 1 h. In presence of ROS, the yellow color NBT reduced to blue black colored formazan, which was dissolved in DMSO after stipulated time period and optical density were measured using microplate reader (BioradiMark^{TM}) at 595 nm.

2.5.4 Lipid peroxidation (LPO) assay

Lipid peroxidation is the degradation of lipids that occurs as a result of oxidative damage and is a useful marker for oxidative stress (Ayala et al., 2014). Polyunsaturated lipids are susceptible to an oxidative attack, typically by reactive oxygen species, resulting in a well-defined chain reaction with the production of end products such as malondialdehyde (MDA) and 4-hydroxynonenal (4- HNE). These end products are often used as markers of LPO, and to assay for oxidative damage / oxidative stress. LPO is determined by the reaction of MDA with thiobarbituric acid (TBA) to form a colorimetric (532 nm)/fluorometric (λex = 532/λem = 553 nm) product (MDA-TBA adduct), proportional to the MDA present.

Here, LPO is evaluated in terms of MDA, which is determined spectrophotometrically at 532 nm. The released MDA is toxic in nature, which damages the bacterial DNA and protein. Initially, the HA and HA – x Au/Ag NPs (x=2, 5 and 10 wt. %) composite samples were cultured with bacterial cells (*E. coli* and *S. aureus*) and incubated for 8 h. Thereafter, lysozyme (1 mg/mL) was added and further incubated for 1 h. After incubation, centrifugation was done for 10 min, at 10 000 rpm in4 ℃ and the supernatant was collected. Then, 500 μL of Tris-HCl was mixed with 500 μL of as collected supernatant in a test tube and incubated for 2 h at 37 ℃. Subsequently, 1000 μL of trichloroacetic acid was added, and centrifuged at 3500 rpm for 10 min. Following this, 1.5 mL of centrifuged solution was mixed with an equal volume of TBA and boiled at 100 ℃ for 10 min. After that, 1 mL of distilled water was added, and absorbance was taken at 532 nm. The LPO activity was calculated in terms of MDA/mg protein using the formula (Eq. 2.9) (Garcia et al., 2005)

$$\textbf{MDA/mg protein} = \frac{\textbf{OD 532}\times\textbf{reaction Volume}\times 10^{9}}{\textbf{Sample volume}\times\textbf{1000}\times\textbf{Extinsion coefficientof MDA}} \qquad (2.9)$$

The extinction coefficient of MDA was taken to be 1.56 × 105 $M^{-1}cm^{-1}$ (Wills et al 1969).

2.5.5 Catalase assay

Catalase is an important antioxidant enzyme responsible for the degradation of reactive oxygen species, hydrogen peroxide (H_2O_2) into water and oxygen (Das and Roychoudhury 2014). The catalase assay quantifies the activity of the catalase enzyme, by measuring hydrogen peroxide (H_2O_2) dissociation spectrophotometrically at 240 nm. Briefly, 100 µL of centrifuged bacterial culture (having enzyme) was mixed with 1.9 mL of phosphate buffer (pH 7.0), followed by addition of 30 mM H_2O_2 (substrate). Thereafter, the absorbance was taken spectrophotometrically at 240 nm. The dissociation of substrate i.e., H_2O_2 by the bacterial cells (containing enzyme), cultured on HA and HA – x Au/Ag NPs (x=2, 5 and 10 wt. %) composite surfaces, was calculated in terms of catalase activity/second (Eq. 2.10) (Chance et al., 1995)

$$\textbf{Catalase activity } (\mathbf{K}) = \frac{\mathbf{2.3}}{\mathbf{\Delta t}} \times \mathbf{log}\frac{\mathbf{E_1}}{\mathbf{E_2}} \qquad (\mathbf{2.10})$$

Where, E_1 and E_2 represent the absorbance at t = 0 and t = 30 s, respectively.

2.5.6 Protein estimation

In this assay, first of all reagent A (consisting of 0.1 NaOH and 2 % Na_2CO_3) and reagent B (comprises of 0.5 % $CuSO_4$ and 1.35 % potassium sodium tartrate) were mixed in proportion of (48 % of regent A and 2 % of regent B) to make reagent C. After that 20 µl supernatant of centrifuged culture was mixed with 980 µl of D.W., following this 5 ml of reagent C was added to this solution and incubated for 10 min. at room temperature. Then 500 µl of follins regent was added and incubated further for 30 min. that change the

colour of solution to blue which is measured spectrophotometrically at 750 nm. Thus, obtained absorbance is directly proportional to the protein concentration.

2.5.7 Minimum Inhibitory Concentration (MIC) determination

Minimum Inhibitory Concentration (MIC) test determines the lowest concentration of an antimicrobial agent that hinders the visible growth of micro-organisms in a culture medium. This test is used to evaluate the efficacy of novel antimicrobial drugs and other antimicrobial-treated compounds against bacteria.

The minimum inhibitory concentration of Cur, AuNPs, Cur-AuNPs, CEO-*f*AuNP was determined by the broth microdilution method as described earlier with minor modifications (Singh et al 2017). Briefly, *Klebsiella pneumonia* (MDR) were grown in 10 ml BHI broth aerobically for 18 h. Bacterial culture (500 µl) was then diluted to 1.5 ml fresh BHI broth. The stock solution of Cur, AuNPs, Cur-AuNPs, CEO-*f*AuNP were diluted in a series of two-fold dilutions ranging from 0.5 to 512 µg/ml in sterile BHI broth in microtiter wells. Each well of the 96-well microtiter plate was then inoculated with 190 µl of standardized cell suspension (10^5 CFU/ml) and incubated at 37 °C for next 18 h along with the 20 µl Cur, AuNPs, Cur-AuNPs, CEO-*f*AuNP diluted solution. The MIC was defined as the lowest concentration of Cur, AuNPs, Cur-AuNPs, CEO-*f*AuNP at which no obvious growth was observed.

2.5.8 Bacterial growth reduction analysis

The Time-kill kinetics assay is used to study the activity of an antimicrobial agent against a bacterial strain and can determine the bactericidal or bacteriostatic activity of an agent over time. We used spectrophotometry to track how Cur, AuNPs, Cur-AuNPs and CEO-*f*AuNP affected the growth rates of the respective bacteria as previously described (Singh et al., 2019). In a summary, overnight-grown bacterial cells were allowed to grow to their

early exponential phase in fresh BHI broth. Once accomplished, the bacteria-containing broth was inoculated into a tissue culture plate with an initial absorbance of 0.01 at a wavelength of max 600 nm. After 2 h, change in absorbance of each well was assessed to evaluate the effects of the intervention.

2.5.9 Membrane dynamics

1,6-Diphenyl-1,3,5-hexatriene (DPH) is one of the most commonly used fluorescent probes to study dynamical and structural properties of lipid bilayers and cellular membranes via measuring steady-state or time-resolved fluorescence anisotropy (Poojari et al., 2019). DPH interacts with acylated lipids of the cell membrane, therefore intercalates in it, and hence fluoresce (Yadav et al., 2020). However, if the membrane integrity is compromised, insertion of DPH into the membrane does not take place, and hence its fluorescence is also forfeited. We assessed it using flow cytometry.

We studied change in membrane dynamics as described earlier (Singh et al., 2019). With MIC concentrations of Cur, AuNPs, and Cur-AuNPs, multidrug-resistant *Klebsiella pneumoniae*tes isolate were treated for 120 min with shaking (170 rpm) at 37°C, with subsequent harvesting. The pellet was re-suspended and re-pelleted. The final pellet was fixed with0.4% paraformaldehyde with subsequent resuspension in PBS (pH 7.2). The re-suspended cells were then pelleted and thoroughly washed thrice with PBS before being treated with 0.5 mM 1, 6-diphenyl-1, 3, 5-hexatriene (DPH) for 60 min at 37°C. Flow cytometry (C6 BD Accuri, Becton-Dickinson, San-Jose, CA, USA), was used to evaluate the percentages of bacterial cells exhibiting fluorescence response.

2.5.10 DCFH-DA (ROS)

$DCFH_2$-DA (2′,7′-dichlorodihydrofluorescein diacetate) is the most widely used fluorogenic probe for the detection of general oxidative stress (Reiniers et al., 2017). The

DCFDA assay protocol is based on the diffusion of DCFDA / H_2DCFDA / DCFH-DA / DCFH into the cell. It is then deacetylated by cellular esterases to a non-fluorescent compound DCFH, which is later oxidized by ROS into 2', 7' –dichlorofluorescein (DCF) (Figure 2.10). DCF is highly fluorescent and is detected by fluorescence spectroscopy with excitation / emission at 485 nm / 535 nm.

Endogenous reactive oxygen species (ROS) production in bacteria after the exposure of Cur, AuNPs, Cur-AuNPs for 48 h was monitored by flow cytometry using 2′, 7′-dichlorofluorescein-diacetate (DCFH-DA) as ROS marker described earlier (Singh et al., 2018). The bacterial cells were pelleted after being exposed for 2h to Cur, AuNPs, and Cur-AuNPs. They were then washed thrice with PBS (pH 7.2), and their density was adjusted to 10^7/ml by suspending them in PBS. The resuspended cells were then incubated with 5 M DCFHDA for 30 min, after which the ROS generation was measured using a BD Accuri C6 Flow cytometer.

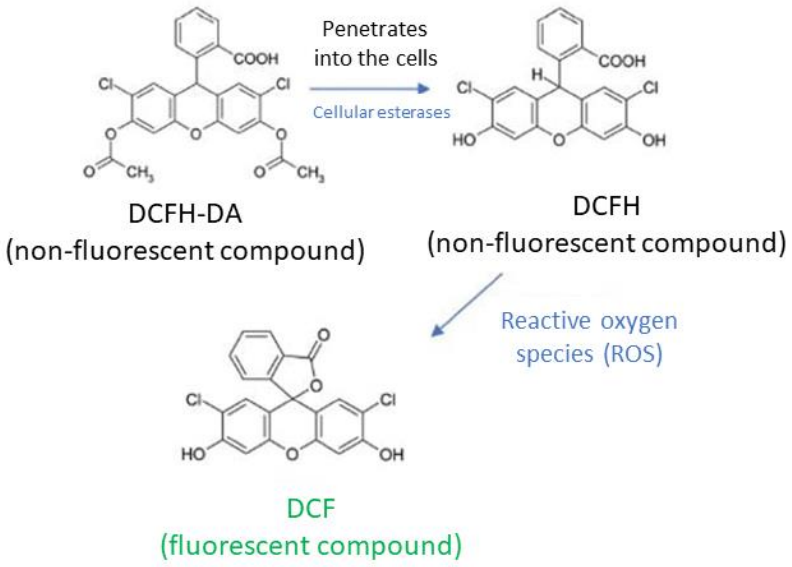

Figure 2.10 *The formation of DCF from DCFH_2-DA.*

Based on light-scatter and fluorescence signals generated by 20mW laser illumination at 488 nm, the data was acquired using the BD Accuri C6 software. Logarithmic calculations were used for all measurements. The assay was performed at a low sample rate (14-µl min^{-1}). A total of 10^6 events were considered for each sample.

2.6 Antibiofilm

2.6.1 Antibiofilm activity determination by Crystal Violet

The antibiofilm assay was performed utilizing semi-quantitative CV assay in 96-well tissue culture plate described previously (Singh et al., 2017). Briefly, the overnight culture of *Klebsiella pneumoniae*, was grown in Luria Bertani broth. The 20 µl of diluted bacterial suspension (0.5 McFarland's) was suspended in flat-bottom polystyrene 96-well tissue culture plate and 180 µl of Cur, AuNPs, Cur-AuNPs and CEO-*f*AuNP were added to each well. Wells without these compounds were set up as negative controls while positive control wells contained imipenem (200 µg/ml). Plates were incubated at 37°C without shaking for 48 h to investigate its biofilm inhibitory potential. The biofilm inhibition was quantified by crystal violet (CV) assay as percentage reduction in its biomass content as described earlier (Eq. 2.11).

$$\% \textbf{ Reduction} = \frac{(\textbf{OD 570 control} - \textbf{OD 570 sample})}{\textbf{OD 570 control}} \textbf{x 100} \qquad \textbf{(2.11)}$$

2.6.2 Confocal laser scanning microscopic (CLSM) evaluation of the antibiofilm activity of Cur, AuNPs and Cur-AuNPs

Confocal microscopy was used to directly observe how Cur, AuNPs, and Cur-AuNPs affected the bacterial viability. For this, we grew *K. Pneumonia* in chambered slides as described previously with modifications (Singh et al., 2021). In an 8-well flat-bottom

chambered slide with 450 µl of BHI broth added with 4% glucose was dispensed with 50 µl of the diluted bacterial suspension. After that it allowed to grow statically for 72 h at 37 °C. The solution was then treated (20 µl (MIC conc.) of Cur, AuNPs, and Cur-AuNPs and observed. Before staining by Concanavalin A tagged with Texas Red (Con A-TR), the chambered slide was gently taped to get rid of any residual broth and cleansed thrice with PBS (pH 7.5) to remove the planktonic cells. Paraformaldehyde (PFA) at 4% (vol/vol) was used to fix the biofilm for 30 min. The top surface of biofilm was superimposed with 50 µl of the reconstituted Con A-TR (10 µg/ml). The Zeiss LSM 880 inverted confocal laser-scanning microscope (Carl Zeiss, Jena, Germany) was used to detect red fluorescence from the dye. Images were obtained via a Plan-Neofluar 40X/1.3 oil objective with a z-step of 2.0 µm or 20 × objective with a z-step of 5.0 µm and analysed through Zen Black software.

2.7 Antioxidant activity (DPPH free radical assay)

The 2,2-Diphenyl-1-picrylhydrazyl (DPPH) is a popular, quick, easy, and affordable approach for the measurement of antioxidant properties that includes the use of the free radicals used for assessing the potential of substances to serve as hydrogen providers or free-radical scavengers (FRS). The technique of DPPH testing is associated with the elimination of DPPH, which would be a stabilized free radical. The free-radical DPPH interacts with an odd electron to yield a strong absorbance at 517 nm, i.e., a purple hue. An FRS antioxidant, for example, reacts to DPPH to form DPPHH, which has a lower absorbance than DPPH because of the lower amount of hydrogen (Figure 2.11). It is radical in comparison to the DPPH-H form, because it causes decolorization, or a yellow hue, as the number of electrons absorbed increases. Decolorization affects the lowering capacity significantly. As soon as the DPPH solutions are combined with the hydrogen

atom source, the lower state of diphenylpicrylhydrazine is formed, shedding its violet colour.

DPPH free radical method is an antioxidant assay based on electron-transfer that produces a violet solution in ethanol. This free radical, stable at room temperature, is reduced in the presence of an antioxidant molecule, giving rise to colourless ethanol solution. The use of the DPPH assay provides an easy and rapid way to evaluate antioxidants by spectrophotometry.

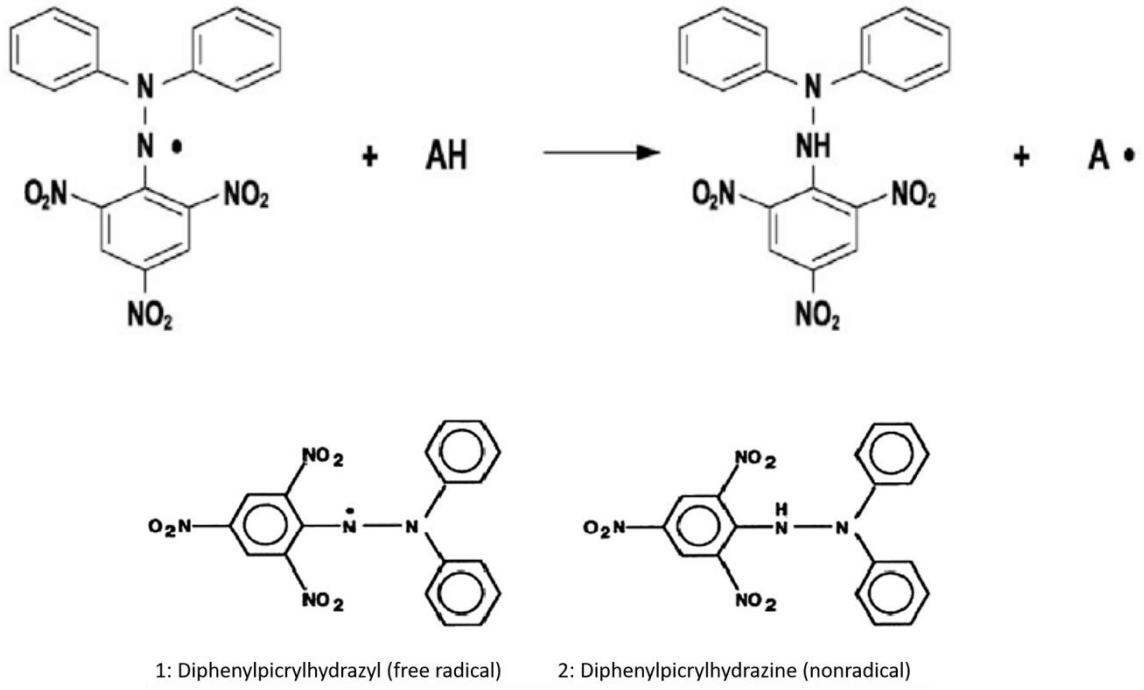

Figure 2.11 *DPPH radical and its stable form*

The assay is based on the measurement of the scavenging capacity of antioxidants towards it. The odd electron of nitrogen atom in DPPH is reduced by receiving a hydrogen atom from antioxidants to the corresponding hydrazine. On mixing DPPH solution with a substance that can donate a hydrogen atom, it gives rise to the reduced form with the loss of violet colour. Representing the DPPH radical by Z• and the donor molecule by AH, the primary reaction is (Eq. 2.12).

$$\mathbf{Z^* + AH \rightarrow ZH + A^*} \qquad \mathbf{(2.12)}$$

Where ZH is the reduced form and A• is free radical produced.

The antioxidant efficacy of CEO and CEO-*f*AuNP was evaluated by a DPPH assay with minor modifications (Das et al., 2014). The presence of an antioxidant molecule scavenges DPPH free radicals, reducing the purple-coloured stable radical cations to a yellow-coloured solution with a consequent decrease or loss of absorbance, which can be measured via a spectrophotometer.

In brief, 0.3 ml of methanolic solution of DPPH (0.5mM) was added to different concentrations of CEO and CEO-*f*AuNP; and incubated in the dark for 100 min. The optical density post-reaction completion was measured using a UV-Vis spectrophotometer at 517 nm. The experiment was repeated thrice ensure reproducibility. The antioxidant efficacy against the DPPH free radical was calculated using the following equation 2.13:

$$\textbf{Antioxidant activity } (\%) \quad = \frac{\mathbf{A_{control}\,(A_{CEO-fAuNP} - A_{correction})}}{\mathbf{A_{control}}} \mathbf{x\ 100} \qquad \mathbf{(2.13)}:$$

Here, $A_{correction}$ is the absorbance of CEO-*f*AuNP without DPPH and $A_{control}$ is the absorbance without CEO-*f*AuNP addition.

2.8Cell culture experiment

To evaluate the in vitro cytocompatibility of AuNPs, Cur-AuNPs, CEO-*f*AuNPs, HA and HA-xAu/Ag NPs composite samples, osteoblast cells (MG-63, NCCS, Pune) were cultured in Dulbecco's modified Eagle's medium (DMEM), supplemented with 15 % fetal bovine serum (FBS) and 1 % antibiotics, and incubated in a humidified CO_2(5 %) incubator (Thermo scientific Heracellvios 160i CO_2 incubator) at 37ºC. Before seeding, the samples as well as control disk were autoclaved at 121°C and 15-pound pressure for 15 min. Following this, the samples were soaked in 70% ethanol along with UV exposure

for 1 h, followed by washing with 1X PBS. After sterilization, the cells were trypsinised and an equal amount of cells (10^4cells/ml) were seeded on glass disc (control), Cur-AuNPs, CEO-*f*AuNPs, and HA-xAu/Ag composites in 24 well plates for 30 min. Subsequently, 500 µL growth media was added to each well and incubated further in CO_2 incubator. Media was changed every 48-72 h. All the experiments were performed in triplicates for 3 days, 5 days and 7 days.

2.8.1Quantitative analyses (MTT assay)

MTT method is one of the most widely used methods to analyze cell proliferation and viability. The MTT assay is a colorimetric assay for measuring cell metabolic activity. It is based on the ability of nicotinamide adenine dinucleotide phosphate (NADPH)-dependent cellular oxido-reductase enzymes to reduce the tetrazolium dye MTT to its insoluble formazan, which has a purple colour (Figure 2.12). This assay therefore measures cell viability in terms of reductive activity as enzymatic conversion of the tetrazolium compound to water insoluble formazan crystals by dehydrogenases occurring in the mitochondria of living cells although reducing agents and enzymes located in other organelles, such as the endoplasmic reticulum are also involved (Lu et al., 2012; Stockert et al., 2012).

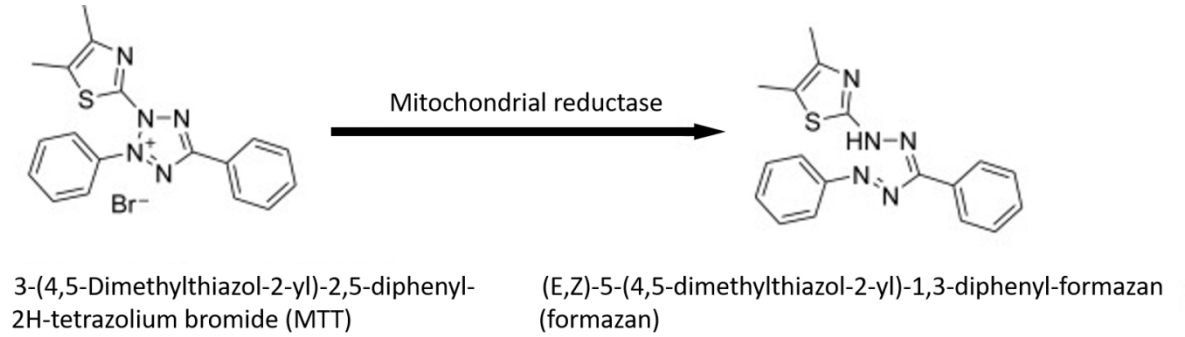

Figure 2.12 *Conversion of the tetrazolium salt MTT into formazan dye in presence of mitochondrial reductase.*

In the MTT assay, a solubilisation solution (dimethyl sulfoxide or acidified ethanol solution, or a solution of the detergent sodium dodecyl sulfate in diluted hydrochloric acid) is added to dissolve the insoluble purple formazan product into a colored solution. The absorbance of this colored solution can be quantified by measuring at a certain wavelength (usually between 500 and 600 nm) by a spectrophotometer. MTT is taken up through endocytosis and is reduced by mitochondrial enzymes as well as endosomal/ lysosomal compartments, and then it is transported to cell surfaces to form needle-like MTT formazans (Lu et al., 2012).

Cell viability was assessed by MTT assay. The cells, seeded on HA and HA-xAu/Ag NPs composite samples were incubated for 3, 5, and 7 days in CO_2 incubator. In case of AuNPs, Cur-AuNPs, CEO-*f*AuNPs; cells were seeded (10,000 cells/well) in 96-well tissue culture plates and incubated overnight, followed by replacement of media with 100µl of test samples (MIC conc. of AuNPs, Cur-AuNPs, CEO-*f*AuNP) in fresh culture media and cytotoxicity was monitored at the intervals of 3, 5 and 7 days. After respective incubation period, the cells were washed with 1x PSB and 500µL MTT (reconstituted 5mg/ml in 1x PBS) with DMEM without phenol red in 1:10 dilution was added and incubated further for 6 h to form formazan crystals. The crystals were dissolved in DMSO and optical density was measured at 590nm using microplate reader (BioradiMark^{TM}).

2.8.2Morphological analysis

Cells, seeded on HA and HA-xAu/Ag NPs composite samples as well as cells treated with MIC conc. Of AuNPs, Cur-AuNPs were fixed in 4% paraformaldehyde at 4°C for 30 min, followed by permeabilization with 0.1% triton X 100 (in 1x PBS) for 10 min. Then blocking was performed using 1% Bovine Serum Albumin (BSA) in 1x PBS for 1 h

at 4°C. After blocking cells were incubated with Alexa Flour 488 Phalloidin (Invitrogen) diluted in 1% BSA in ratio of 1:500 for 1 h to stain cytoskeleton, whereas Hoechst dye (Invitrogen) were used to stain nuclei in dilution of 1:5000 with 1x PBS for 10 min. Proper washing (2-3 times) of the samples were done using 1x PBS after every step. The stained cells were observed under fluorescent microscopy (Nikon Eclipse LV 100ND) for cell morphology and cell density quantification.

2.9Conclusion

As a closure, this chapter demonstrated the synthesis of AuNPs,Cur-AuNPs, CEO-fAuNP, Hydroxyapatite (HA), Gold/Silver bimetallic nanoparticles (Au/Ag NPs), and (1-x)HA - x Au/Ag NPs composites. The Phase evolution and microstructural analyses were done using XRD, FTIR, TEM, DLS and Zeta potential, respectively. Mechanical characterization (hardness, fracture toughness, flexural and compressive strength of (1-x)HA - x Au/Ag NPs composites were carried out to show the mechanical stability of the material. The antibacterial nature have been assessed using MIC determination, time-dependent bacterial killing, and antibiofilm activity mechanisms underlying their antimicrobial effects, including disruption of cell membranes reactive oxygen species (ROS) generation and interference with biofilm formation. In addition, the cell culture tests in terms of quantitative as well as qualitative were performed to observe the biocompatibility of synthesized of AuNPs,Cur-AuNPs, CEO-*f*AuNP, Hydroxyapatite (HA), Gold/Silver bimetallic nanoparticles(Au/Ag NPs), and (1-x)HA - x Au/Ag NPs composites.